Acta Neuropathol (2002) 103:255–266
DOI 10.1007/s004010100463

REGULAR PAPER

Dietmar Krex · Martin Hauses · Hella Appelt
Brigitte Mohr · Gerhard Ehninger
Hans Konrad Schackert · Gabriele Schackert

Physical and functional characterization of the human *LGI1* gene and its possible role in glioma development

Received: 2 May 2001 / Revised, accepted: 16 August 2001 / Published online: 8 December 2001

Abstract The human gene termed *LGI1* (leucine-rich gene – glioma inactivated) has been isolated recently, and is supposed to be an additional candidate tumor suppressor gene involved in the formation and progression of glioblastoma multiforme [Chernova et al. (1998) Oncogene 17:2873–2881]. To test this hypothesis and to complete the characterization of the gene, we performed various detailed studies on the genomic structure, the mRNA expression level, the integrity of the cDNA, and retroviral gene transfer into *LGI1*-deficient cell lines. Two single nucleotide polymorphisms in the promotor region and a highly polymorphic intragenic microsatellite repeat between exon 4 and 5 were found. Phylogenetic sequence analysis techniques were applied, which showed functional relationships between LGI1 and TRK and SLIT protein families that are known to be involved in development and maintenance of the nervous system. Fluorescence in situ hybridization (FISH) analysis showed *LGI1* to be present on 10q24 in each of 11 glioma-derived cell lines evaluated. Sequence analysis of the *LGI1* transcript did not detect any mutation. Relative amounts of *LGI1* mRNA copy numbers as measured by the real-time fluorescence detection LightCycler technology differed more than three orders of magnitude and were significantly reduced in 10 of 11 cell lines. Retroviral gene transfer into *LGI1*-deficient glioma-derived cell lines could not substantiate any difference to control infected cultures regarding growth rate, S phase transition, and maintenance of marker gene expression. The strong homology to proteins involved in development, differentiation, or maintenance of the nervous system provides evidence for a function of the LGI1 protein in neural tissue. The observation that translocation or deletion of the *LGI1* locus or mutation of the coding sequence of the *LGI1* mRNA is not a frequent event in malignant glioma cell lines suggests that epigenetic factors lead to substantial differences in the amount of *LGI1* mRNA expression. In addition, that the effect is lacking after retroviral gene transfer in cell culture suggests that binding of some kind of a ligand is essential for its biological activity.

Keywords LGI1 · Glioblastoma · Pathogenesis · Tumor suppressor · Gene

The first two authors contributed equally to this study

D. Krex (✉) · M. Hauses · G. Schackert
Department of Neurosurgery,
Universitätsklinikum Carl Gustav Carus,
University of Technology, Dresden,
Fetscherstrasse 74, 01307 Dresden, Germany
e-mail: krex@rcs.urz.tu-dresden.de,
Tel.: +49-351-4582886, Fax: +49-351-4584304

B. Mohr · G. Ehninger
Department of Internal Medicine/Hematology and Oncology,
Universitätsklinikum Carl Gustav Carus,
University of Technology, Dresden, Germany

H. Appelt · H.K. Schackert
Department of Surgical Research,
Universitätsklinikum Carl Gustav Carus,
University of Technology, Dresden, Germany

Introduction

Genetic derivations involving chromosome 10 seem to play a decisive role in the pathogenesis of glioblastoma multiforme, which represents the most common primary intra-axial brain tumor in adulthood [19, 26, 42]. Loss of heterozygosity (LOH) for *PTEN/MMAC1*, a well-characterized tumor suppressor gene (TSG) located at 10q23, was found to be present in about 70% of tumor tissues of malignant gliomas [29]. Mutations of the coding sequence occur in approximately 30% of glioblastomas but are rare in lower grade astrocytomas [10], suggesting that loss of PTEN/MMAC1 function is a late event in the pathogenesis of gliomas [52]. Furthermore, LOH at the *PTEN/MMAC1* locus seems to be correlated with a poor prognosis [41].

LOH of *DMBT1*, another candidate TSG located at 10q25.3-26.1, is frequently found in equal amounts in both low-grade and high-grade astrocytomas [29, 33]. Therefore, this seems to be an early event in glioma

pathogenesis. The overall frequency of rearrangements and deletions found for the entire 10q-ter region in glioblastomas suggests that there are other TSGs in that genomic region [20, 37].

Other candidate TSGs have been proposed such as *MXI1* [48] and *h-neu* [34], both located at 10q25.1. In the case of *MXI1*, sequence analysis in glioblastoma tissues has been performed, but no somatic mutations were found, while induction of the gene's expression in a *MXI1*-deficient glioma cell line resulted in a decreased growth rate, suggesting that *MXI1* may play a role as a TSG in astrocytomas [49].

Recently, another gene termed *LGI1* (leucine-rich gene – glioma inactivated) was mapped to 10q24 between *PTEN/MMAC1* and *DMBT1* [5]. The gene was found to be rearranged or translocated in two glioma cell lines, leading to a complete absence of *LGI1* expression as far as this is detectable by conventional reverse transcription (RT)-PCR. Expression of mRNA was high in different areas of normal brain, while in low-grade astrocytomas expression was reduced and almost absent in glioblastomas when analyzed by Northern blotting and RT-PCR. Localization, rearrangement, and the distinctive expression of *LGI1* in low- and high-grade astrocytomas, and in the normal brain suggest that this gene represents another candidate TSG involved in the malignant progression of glial tumors [5].

To test the hypothesis that *LGI1* is a TSG, we performed various studies to complement previous gene characterization [5, 43]. We analyzed the genomic structure of *LGI1* including the intron sequences. Beside sequence comparison, the conservation of intron positions within genes or functional domains is a useful criterion to gain information about their relationships. It is increasingly recognized that individual intron positions typically show a restricted phylogenetic distribution [8, 9, 30]. We studied the integrity of the gene at the chromosomal and mRNA level to determine inactivation and lowered expression, which are essential features of a TSG. Common reasons for inactivation include genomic deletions and/or mutations, leading to the loss of a functional protein. However, there is increasing evidence that other mechanisms like transcriptional inactivation also can contribute to TSG inactivation [14, 39].

Furthermore, the analysis of genetic variants, whether they affect coding sequences or not, is attracting increasing interest due to their potential use in diagnosis or treatment of diseases. We have analyzed the promotor region for sequence variants and we have discovered a highly polymorphic intragenic dinucleotide repeat. Finally, re-expression of a gene in cell culture is widely used for investigating whether a gene can change growth, differentiation and cell cycle in vitro, which is a prerequisite for further in vivo studies.

Material and methods

Cell culture

Cell lines T17, A172, U343, U373, T406, T508, T1115, and Hero were kindly provided by the laboratory of R. Fischer (German Cancer Research Center, Heidelberg, Germany). U87-MG cells were obtained from ATCC (Manassas, Va.). H4 cells were kindly provided by J. Mollenhauer (German Cancer Research Center) and HS683 cells by R. Reszka (Max-Delbrück-Center, Berlin, Germany).

Cell lines were maintained in BME supplemented with 2 mM L-glutamine, 50 mM HEPES, 10% fetal bovine serum (all media and supplements from Gibco BRL Life Technologies, Karlsruhe, Germany) in 5% CO_2 at 37°C. There were no antibiotic supplements used in the media.

Cloning of the *LGI1* gene and generation of a *LGI1* and *PTEN/MMAC1* locus-specific hybridization probe

A cDNA clone harboring the entire open reading frame (ORF) of *LGI1* was generated in a PCR reaction using primers GT13s and GT14a (Table 1) and I.M.A.G.E. cDNA clones IMAGp998B24161 and IMAGp998015326 [Resource Center/Primary Database (RZPD) of the German Human Genome Project, Berlin, Germany] as template. The PCR product was cloned into the pCR 2.1-TOPO vector (Invitrogen Corp. Carlsbad, Calif.) and sequenced. The *Eco*RI excised insert was used by the RZPD as a hybridization probe to screen human P1 and PAC libraries for

Table 1 Primer list. PCR primers used in conventional and LightCycler PCR for cDNA sequence analysis, quantification, and microsatellite analysis

Primer	Sequence (5' – 3')
GT1s	CATTGCTGGAGCGAGGAGAA
GT2a	GAGCTGCAGCGATGGCGTGA
GT3s	CGAACTCCTTTGATGTGATC
GT4a	CTTCGCAGTAGATGTCTTCA
GT5s	GGACCATGTGGACAAGACCT
GT6a	CACATCAGTGTCCCTGTACCA
GT7s	GTAATTCATTTAATTGTGACTG
GT8a	TTTCAATGACTATAGGCTTGC
GT9s	TGAATGATGAGTATGTAGTC
GT10a	GTAATCACTTCCAAGAATTGC
GT11s	AAGATTGAAAACAACTGGTAC
GT12a	ACTTCCCACATCACTGGACTG
GT13s	GACAATCACCATCTGAATTC
GT14a	ATTTCTGATGGCAGCCACAG
GT15s	TCCTTTGTGAGATCTGGTTTTAC
GT16a	CTAAGAACAGGTCACATAGGAG
GT17s	CATAGAAAACAACAACATCAAGTC
GT18a	AAATACTCTAGATGTGGAAGAC
GT19s	AACCAAGCACTACCAGTATCTC
GT20a	AAGTGAATTAATGACTTTAGTCC
GT21s	GATGAACTCAATGCATGATGAC
GT22a	TTTCCACATGGTCCCATTCAAG
GT23s	AAACAACAATCTCCAGACACTC
GT24A	CATTTGTTAAAGAATCCAGGCC
GTI7s	GCTCTAAGTCTGAACTGCTTCC
GTPA1	CCGCACTTCTGTTTCCCTTCC
I4MSS1	TTGTTTCTTCTAGCTCCCTCACC
I4MSA1	GTTTGGCAGGATTATTGAGAGG

LGI1-specific genomic DNA [library no.: 700, 704 (RPCI1, 3–5, Roswell Park Cancer Institute, Buffalo, N.Y.), respectively; RZPD]. This hybridization revealed 15 clones, which were rescreened by PCR amplifications (primer sequences listed in Table 1). Clones RPCIP704M101099Q2 and RPCIP704C07989Q2, containing the entire coding region of *LGI1*, were used as hybridization probes for fluorescence in situ hybridization (FISH).

In a similar procedure, a *PTEN/MMAC1* locus-specific hybridization probe was generated. A genomic fragment of the *PTEN/MMAC1* locus spanning exons 4 to 5 was amplified from human genomic DNA by PCR utilizing primers pte4s (5´-tgtgctgagagacattatgac-3´) and pte5a (5´-ttgtctctggtccttacttc-3´). Cloning and screening of the human PAC library was performed as mentioned above. Clone RPCIP704D02401Q2 contained the entire ORF and was used as a hybridization probe for FISH.

Determination of the physical structure of the gene

Fragments of clone ICRFP700M0924Q5 generated by partial restriction enzyme digestion were cloned into pBluescript KS+ (Stratagene, La Jolla, Calif.) and subjected to sequence analysis utilizing T7 or reverse primers. Additionally, fragments of the gene were amplified by PCR in the presence of 100 ng ICRFP700M0924Q5 (PCR conditions on request). Sequence determination was carried out either from subcloned DNA with M13 or T7 primers, from PCR products or directly from clone ICRFP700M0924Q5 using Cy5-labeled primers and Thermo Sequenase Fluorescent Labeled Primer Cycle Sequencing Kit with 7-deaza-dGTP (Amersham Pharmacia, Braunschweig, Germany). Sequencing reactions were resolved on denaturing 6.5% Long Ranger gels (FMC Bioproducts, Rockland, Me.) using an automated laser fluorescence sequencer (ALFexpress, Amersham Pharmacia Biotech). Runs were analyzed using ALF Evaluation software. Contigs were build using the Fragment Assembly System of the GCG package.

Database sequences and computational methods

Database searches were carried out by implementations of the BLAST algorithm [1]. Sequence data of clones RP3-485O9 (accession no. AL136447) and RP4–579A14 (accession no. AL136314) were produced by the human chromosome 6 sequencing group at the Sanger Center. Sequence data of clones RP11-12E5 (accession no. AC013310), 10_P_19 (accession no. AC012142) and RP11-397D2 (accession no. AC021468) were produced by the Whitehead Institute/MIT Center for Genome Research. Sequence data of clone RP11-332D24 (accession no. AC021118) were produced by the Washington University Genome Sequencing Center. Sequence data of clones CTC-229B20 (accession no. AC027311), CTC-279L15 (accession no. AC008409), CTC-392L24 (accession no. AC008479) and CIT-HSPC_558O2 (accession no. AC011365) were produced by the Joint Genome Institute. Multiple sequence alignments were calculated using Pileup [12] with gap weight 8, gap length weight 2 and end gaps penalized like other gaps. Protein distance matrix analysis was performed using the Phylogenetic Interference Package, PHYLIP, Version 3.57c [11]. One hundred bootstrap replications were carried out via the program SEQBOOT. Distance matrices were calculated by PROTDIST in conjunction with Dayhoff's PAM001 matrix. Trees were build according to the UPGMA method of clustering by NEIGHBOR and the consensus tree was created by the Ml method using CONSENSE.

Cytogenetic analysis and FISH

FISH analysis was performed in each cell line using either WCP chromosome paint DNA FISH probes labeled with SpectrumGreen dUTP, or a centromere-specific probe for chromosome 10 (CEP10) alone, or together with the SpectrumRed dUTP (all Vysis GmbH, Bergisch-Gladbach, Germany) labeled *LGI1* locus-specific probe. Furthermore, *LGI1* probes were used together with SpectrumGreen dUTP (Vysis)-labeled *PTEN/MMAC1* probes.

For labeling of *LGI1* and *PTEN/MMAC1* probes, approximately 1 μg extracted PAC-DNA was subjected to nick translation in the presence of SpectrumRed dUTP and SpectrumGreen dUTP, respectively, according to the manufacturer's instructions (Nick translation Kit, Vysis). Probes were precipitated in the presence of COT-1 DNA (Vysis) and placental DNA (Sigma, Deisenhofen, Germany). Preparations of 1×10^7 cells were harvested and prepared for metaphase-FISH according to the manufacturer's protocol (Vysis). Cells were exposed to colcemid; thus metaphase chromosome spreads were hybridized according to standard protocols [35].

RT-PCR, sequencing, and analysis of microsatellite repeats

For mRNA extraction, cells were harvested by trypsination and washed once in cold PBS. The cells were used immediately for the extraction procedure according to QuickPrep Micro mRNA Purification Kit (Amersham Pharmacia Biotech UK, Buckinghamshire, UK). Random hexamer-primed RT was performed using the First-Strand cDNA Synthesis Kit (Amersham Pharmacia Biotech) with an equal amount of mRNA from all cell lines. For amplifying cDNA, 14 primers were used, which are listed in Table 1. For positive control, a β-actin primer pair (5´-cctcgcctttgccgatcc-3´, sense; 5´-ggatcttcatgaggtagtcagtc-3´, antisense) was used that does not co-amplify processed pseudogenes [36]. PCR conditions will be supplied on request. Each run was performed at least in triplicate. Products were resolved on 2% agarose gels and pictured by Eagle-Eye systems (Stratagene). PCR products were quantified from digitalized images by the use of ImageQuant software (Molecular Dynamics, Sevenoaks, UK).

Sequencing of amplified cDNA fragments was performed as mentioned above (Determination of the physical structure of the gene). Microsatellite analysis was performed by multiplex amplification of the microsatellite repeat using 3 pmol of primers I4MSS1 and I4MSA1 together with two products of constant length by primers GT11s and GT10a (exon 8, 474 bp, 3 pmol each) and primers GT7s and GT4a (exon 6, 90 bp, 5 pmol each). PCR products were resolved by electrophoresis on denaturing 6.5% Long Ranger gels as used for sequencing.

Quantification using LightCycler technology

To achieve a relative quantification of *LGI1* expression, the recently developed LightCycler instrument (Roche Molecular Biochemicals, Mannheim, Germany) was used. cDNA of all cell lines was amplified by primers GT1s and GT2a (Table 1), and the β-actin primers, respectively. For online detection of specific amplification products, two labeled hybridization probes were included for *LGI1* and *β-actin*, respectively (6-carboxy-fluorescein phosphoramidite-labeled LGI1FL 5´-cccatccttttgcttctttctgattcca-3´, or actinFL 5´-ggtatgccctcccccatgcc-3´, and 5-carboxy-tetramethyl rhodamine-labeled LGI1LC 5´-cagtcgagaaaatatccccaaccatg-3´, or actinLC 5´-tcctgcgtctggacctggctg-3´; TIB Molbiol, Berlin, Germany).

The reaction mix consisted of 2 μl of cDNA as template, 0.5 μM of GT1s and GT1a primers (Table 1), 0.2 and 0.4 μM, respectively, of each hybridization probe, 4 mM $MgCl_2$, and 1× LightCycler-DNA Master Hybridization Probes (Roche Diagnostics, Mannheim, Germany), in a final volume of 20 μl. The following PCR conditions were used: denaturation for 30 s at 94°C, followed by 45 cycles with denaturation for 5 s at 94°C, annealing for 10 s at 66°C and elongation for 20 s at 72°C. Within each experiment a dilution series of LGI1 and β-actin PCR products was processed as standard. Verification of the correct amplification products was achieved by checking the referring melting curve peaks [38]. Quantitative results were assessed by determination of the cycle threshold value (Ct) as described previously [25]. Relative mRNA levels for *LGI1* and *β-actin* were calculated in relation to the standard dilution series, and LGI1 expression levels were normalized for β-actin values.

Retroviral gene transfer and phenotypical analysis of glioma-derived cell lines

Cell lines U87-MG, U343, T1115, and H4 were used out of our group of 11 glioma-derived cell lines. LGI1 cDNA sequence was cloned into the retroviral vector pCFG5-IEGZ (D. Lindemann, A. Rethwilm, unpublished) using the unique *Eco*RI site, thereby generating an expression cassette containing the LGI1 ORF followed by an internal ribosome entry site (IRES) and the ORF of an enhanced green fluorescent protein (eGFP)-zeocin resistance fusion gene. Amphotrophic retroviral particles were generated by transient transfection of 293 transformed embryonal kidney cells and infections were carried out according to the spin-infection protocol [4] with minor modifications. In brief, viral supernatant supplemented with 4 μg/ml protaminsulfate was added to cells seeded in 24-well plates, and plates were centrifuged for 90 min (1,000 *g*, 32°C). After additional 2.5-h incubation time, medium was changed. Gene transfer efficiency was monitored 48 h later by flow cytometric detection of eGFP expression. Cell cycle analysis was performed by flow cytometric analysis of propidium iodide-stained cells according to standard procedures. Growth of transduced cultures was monitored by using Alamar Blue Assay (Biosource, Camarillo, Calif.) according to manufacturer's instructions. Migration was measured by an in vitro wound healing assay [45, 46].

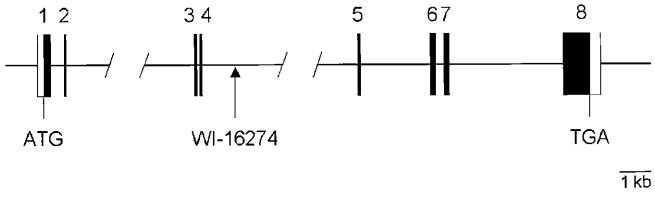

Fig. 1 Schematic view of the *LGI1* gene. The gene is composed of eight exons (1–8), as also reported by Somerville et al. [43]. The start and the end of the coding sequence is marked by ATG and TGA, respectively. The position of the sequence tagged site WI-16274 is marked

Results

Analysis of the human *LGI1* gene

A schematic view of the *LGI1* gene is presented in Fig. 1, and a summary of the gene structure is given in Tables 2, 3. The *LGI1* gene is composed of eight exons. Exon 1 contains the methionine initiation codon and the N-terminal cysteine-rich cluster. Exons 2–5 encode the leucine-rich repeats (LRRs). The C-terminal flanking cysteine-rich sequence is encoded in exon 6. The predicted transmembrane and cytoplasmic domains of the protein are covered by exon 8. These results are in concordance with findings by Somerville et al. [43]. Intron sizes are highly divergent and range from 95 bp to more than 10 kb. All splice donor and splice acceptor sites comply with the GT-AG rule. We identified the sequence tagged site WI-16274 as an intragenic marker. The site is located 1.2 kb downstream of exon 4.

Conserved intron positions in the LRR domain

Determination of the physical structure of the *LGI1* gene revealed that each LRR was interrupted at the fifth amino acid by an intron of variable length. This conserved intron position within the LRRs raised the question, whether this finding is mere a feature of the *LGI1* gene or common to related proteins. Although BLAST searches revealed numerous high-scoring hits for LRR sequences, many fewer genes extended the homologous regions to either the N-terminal or the C-terminal flank. Only two protein families, the TRK family of neurotrophin receptors and genes homologous to *Drosophila slit*, were identified exhibiting homologies within the LRRs and in both flanks. These

Table 2 Summary of the *LGI1* gene intron structure

Intron	splice	donor		splice	acceptor
1	CTCATT	gtaaggcccgtaagc	...	tttgttttctttcag	ATCCTT
2	GCTCTT	gtgagaaatatttat	...	acttttttctgggcag	GTTATT
3	GTATTT	gtaagtaaaaaagct	...	tataacttattgcag	ATTCAT
4	TCACTT	gtaagtatgaatgtt	...	ttttttttttttccag	GAGCCT
5	AAATGT	gtaagaggacctaag	...	aagtttgtctttcag	GGACCT
6	TTACAG	gtaatgtactcatca	...	ttcctatttttgcag	AATTTG
7	TTACAG	gtatgaaaagcctaa	...	tttgtcttttcccag	GCACAT

Table 3 Summary of the *LGI1* gene exon structure

Exon no.	Exon size	Intron						
		Location	Size	Splice donor		Splice acceptor		Amino acid
1	439	439/440	401 bp	ATT	gtaag	ttcag	ATC	Leu
2	72	511/512	10 kb	CTT	gtgag	ggcag	GTT	Leu
3	72	583/584	95 bp	TTT	gtaag	tgcag	ATT	Leu
4	72	655/656	10 kb	CTT	gtaag	tccag	GAG	Leu
5	72	727/728	2.4 kb	TGT	gtaag	ttcag	GGA	Val
6	170	897/898	273 bp	CAG	gtaat	tgcag	AAT	Glu
7	165	1,062/1,063	3,617 bp	CAG	gtatg	cccag	GCA	Gly
8	1,192							

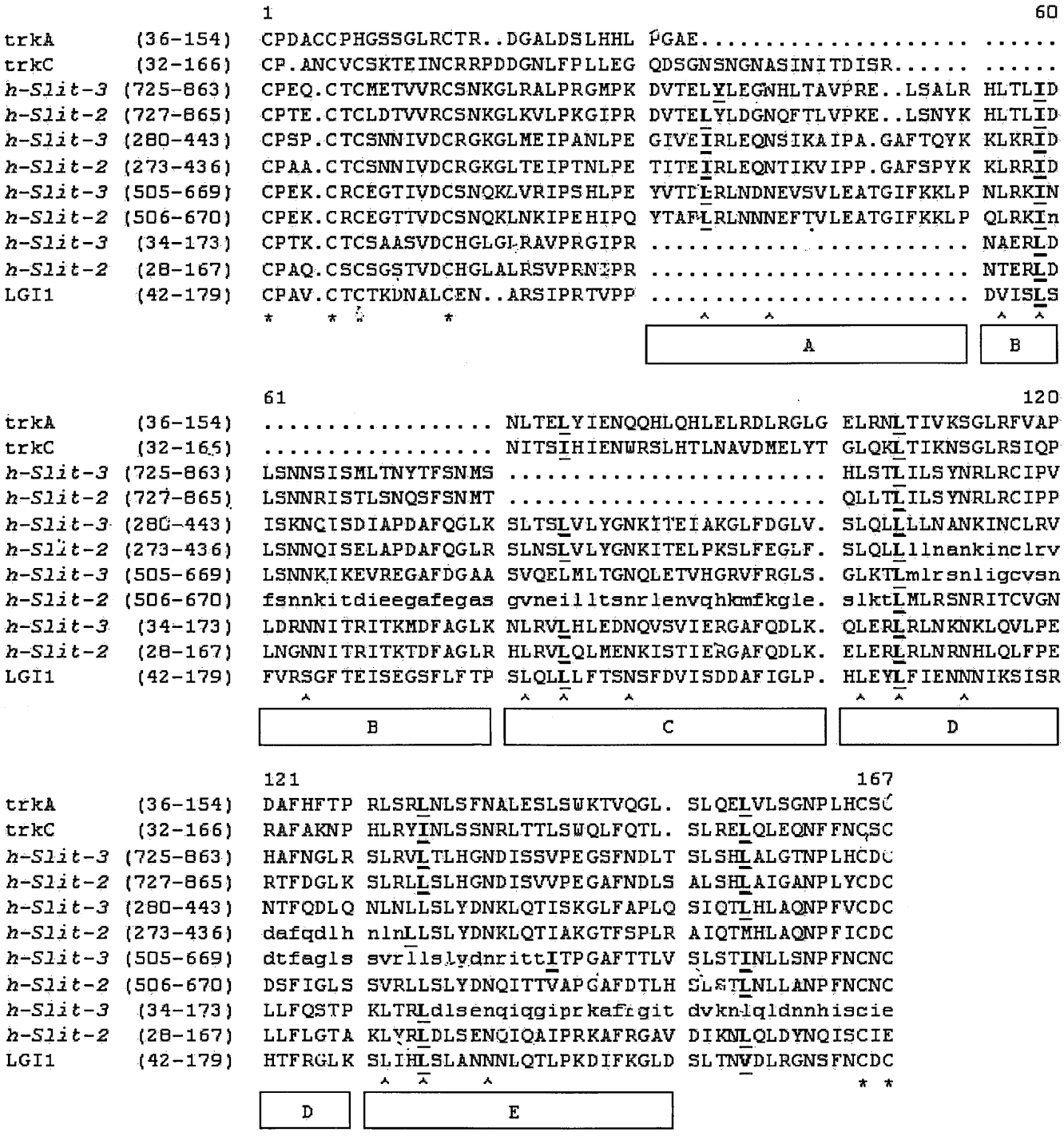

Fig. 2 Multiple alignment of the homologous domains of LGI1 and members of the TRK and h-SLIT protein family. Leucine-rich repeat domains are marked by *boxes* signed with *A–E*. The position where the leucine-rich repeat is interrupted by an intron shown in *bold* and *underlined* amino acid. *Asterisks* indicate cysteine-rich cluster at the N-terminal and C-terminal flank; *small letters* indicate that no genomic sequences are published

homologous regions range from the C-terminal flanking cysteine-rich cluster to the beginning of the N-terminal flanking cysteine-rich cluster.

The N-terminal cluster matches the previously described consensus (CX_3CXCX_6C, where X denotes any amino acid) [3, 24] in all of these proteins with exception of TRKA (CX_3CCX_8C). The C-terminal cysteine-rich cluster of LGI1 perfectly matches the known consensus sequence ($CXCX_{20}CX_{20}C$) [3, 24]. The most extensive difference is found in the N-terminal group of LRRs of the h-SLIT family, where only the first and last cysteine of the C-flank is present ($CX_{47}C$). The other three groups of LRRs within the h-SLIT proteins are highly homologous to the C-flank of LGI1, perfectly matching the consensus

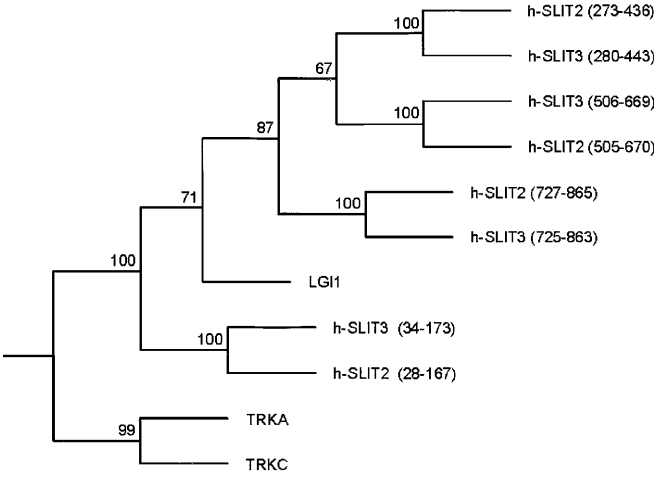

Fig. 3 Phylogenetic tree of LGI1 and members of the TRK and h-SLIT protein family showing a closer phylogenetic relationship of LGI1 with h-SLIT proteins than with TRK proteins. The number of bootstrap replication supporting the note is indicated

$CXCX_{20}CX_{20}C$. The C-flanking cysteine rich cluster of the TRK family follows this consensus with minor numerical aberrations (TRKA: $CXCX_{22}CX_{13}C$; TRKB, TRKC: $CXCX_{22}CX_{17}C$).

The genomic organization of *TRKA* (accession nos. AB019481–AB019488) and *TRKC* (Genebank accession nos. AJ224521–AJ224535) have been identified previously [17]. Exon-intron boundaries of *h-SLIT2* and *h-SLIT3* were determined by aligning the cDNA sequences [18] versus the working draft sequences of human genomic clones. The *h-SLIT2* cDNA produced alignments with clones RP11-332D24, RP11-12E5, RP3-485O9, RP4-579A14 and 10_P_19. Alignments with the *h-SLIT3* cDNA were obtained with clones CTC-229B20, RP11-397D2, CTC-279L15, CTC-392L24 and CIT-HSPC_558O2. These alignments covered the majority of the genes and allowed us to identify the majority of intron positions within the *h-SLIT2* and *h-SLIT3* genes. For *h-SLIT1* and *TRKB*, insufficient genomic sequence was available to include these genes into analysis.

Intron positions within these genes are compared on account of a multiple alignment of the homologous protein domains (Fig. 2). In both analyzed members of the TRK family and in the eight groups of LRRs of h-SLIT2 and h-SLIT3, the prevalent intron position is amino acid five of the individual repeat as seen in LGI1. All repeats of the TRK family demonstrate this pattern, whereas in the h-SLIT family some derivations were noted; four deviations were recognized in h-SLIT3 and three in h-SLIT2. The intron interrupting the first (A) of a group of four repeats formed by amino acids 725–863 of h-SLIT3 is located within codon 6. Within the third repeat (C) of a group of five formed by amino acids 505–669 of h-SLIT3, the intron is missing. The majority of deviations affects the last repeat (E). In two cases (h-SLIT3, 280–443; h-SLIT2, 506–670) the intron is missing. Furthermore, in h-SLIT*2* (273–436) the intron interrupts codon 4 and in h-SLIT3 (506–669) codon 15 of the repeat. The intron generally located at a conserved position in the C-flank is missing in one group of LRRs h-SLIT2 (273–436). Concisely, 48 introns appear in homologous positions in the LRR domains of LGI1, the related domains of the TRK family of neurotrophin receptors and human *SLIT* genes. Only at 7 positions introns are either absent or located at divergent positions.

The observation of substantial homologies of the LRR domains is further substantiated by a comparison of LRR domain sequences using the methods of phylogenetic estimation. The multiple alignment on LRRs was used to build a phylogenetic tree (Fig. 3). Homologous domains of the different h-SLIT proteins always group together, indicating that they may have originated from a single ancestor by an early gene amplification event. Furthermore, the tree shows that LRRs of LGI1 groups together with LRRs of h-SLIT proteins. The LRR domains of TRKA and TRKC show a greater evolutionary distance to LGI1. This observation further strengthens our observation of a close relationship between LGI1 and other proteins involved in development, differentiation, or maintenance of the nervous system.

Cytogenetics and FISH analysis

Eleven glioma-derived cell lines were investigated in this study. To confirm whether chromosome 10 is present and whether there might be structural abnormalities involving chromosome 10, FISH was performed with a probe specific for the entire chromosome 10 (WCP10). An average of 10 mitoses was evaluated, and only distinctly painted chromosomes were counted as positive. All cell lines harbored at least one entire chromosome 10. However, the total number of chromosome 10 copies in 5 out of the 11 cell lines, verified by hybridization with a centromer-10-specific probe (CEP10) in interphase nuclei, was lower than the referring ploidy determined in metaphase spreads.

To analyze whether the *LGI1* locus is retained on chromosome 10 or is a target for deletion or translocation, FISH analysis with a locus-specific probe for *LGI1* was performed. To ensure the association of the *LGI1* signal with the 10q24 region, either the WCP10 or CEP10 probes, or a probe specific for the *PTEN/MMAC1* locus was included in the hybridization reaction. Positive signals for the *LGI1* locus at the 10q24 region were detected in all cell lines (Fig. 4A). Positive spots for *LGI1* loci corresponded with the total number of chromosomes 10, as marked by the CEP10 probe. Furthermore, *LGI1* hybridization signals were only detected on chromosome 10 and never found to be translocated to any other chromosome, as shown by simultaneous hybridization with the CEP10 and WCP10 probes (Fig. 4B). Cell lines T508 and H4, known to have the *PTEN/MMAC1* locus deleted (data not shown), presented a positive *LGI1* signal at 10q, whereas *LGI1* was located telomeric to the *PTEN/MMAC1* locus in all other cell lines studied, suggesting that *LGI1* is not a frequent target for translocations or deletions.

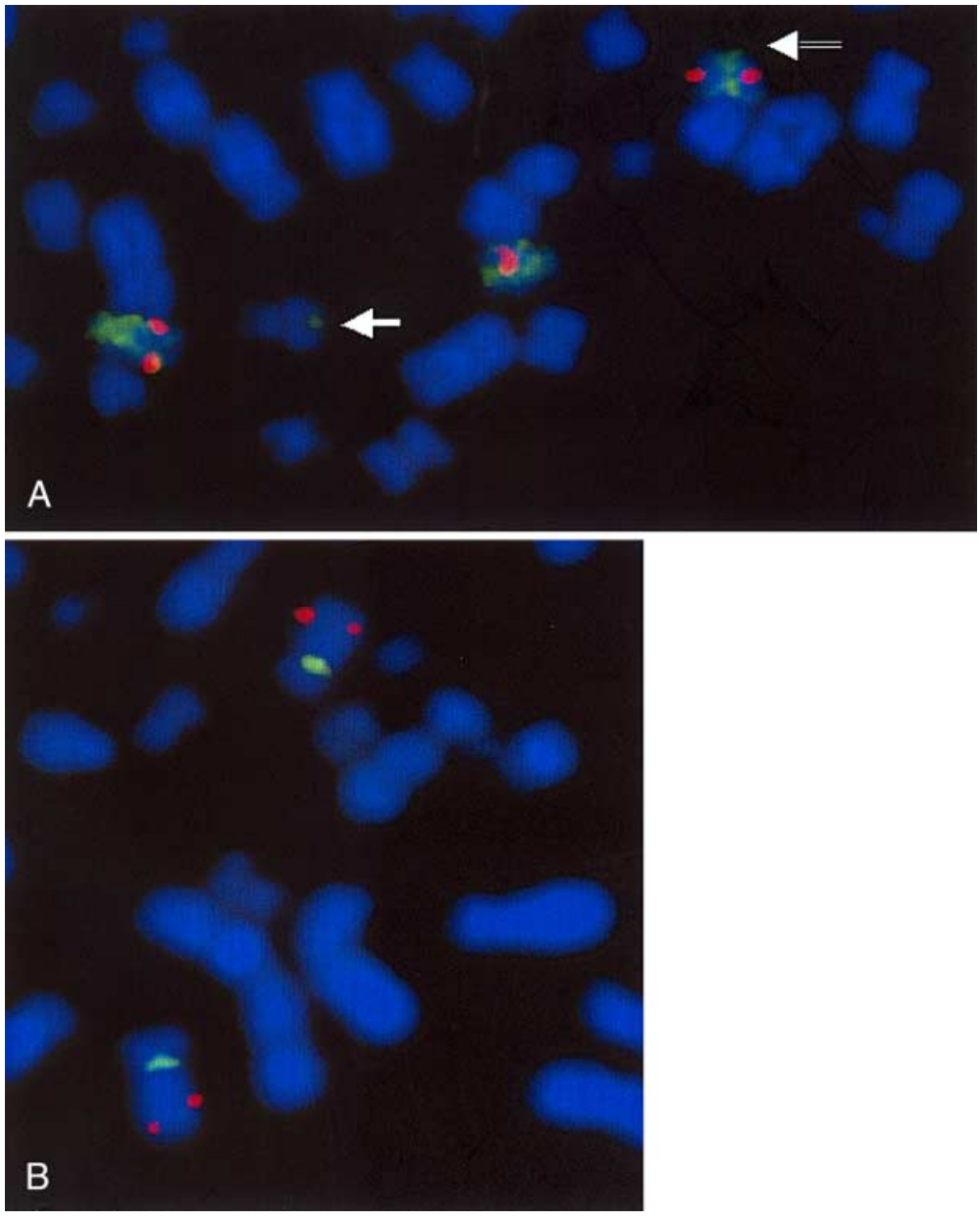

Fig. 4 FISH analysis of cell line H4 (**A**), and T406 (**B**), using different hybridization probes. **A** Cell line H4, hybridized with the WCP10 probe together with the LGI1 locus-specific probe shows a translocation of parts of chromosome 10 to a C-type chromosome (*arrow*) as well a derivative chromosome 10 with loss of 10p (*arrowhead*). The *LGI1* locus is marked by two *red spots* on each chromosome 10. **B** Hybridization of the centromer-specific probe for chromosome 10 (CEP10) (*green*) together with the *LGI1* probe (*red*) revealed the retaining of the *LGI1* locus on both chromosomes 10 in cell line T406 (*FISH* fluorescence in situ hybridization)

Sequencing of *LGI1* transcript and analysis of genetic variants within the *LGI1* gene

To investigate whether the *LGI1* transcript harbors mutations, we used the direct sequencing technique of amplified RT-PCR products. We obtained a positive signal after mRNA isolation, reverse transcription, PCR amplification and gel electrophoresis in ten of our cell lines, while one cell line (H4) did not express any detectable mRNA by this method. The entire ORF of all cell lines was analyzed in various primer combinations and was found to be free of mutations in all ten *LGI1*-expressing cell lines. These results indicate that the *LGI1* locus seems to be transcribed into an intact mRNA in most cases.

To analyze the promotor region of the *LGI1* gene, a DNA fragment was amplified using primers GTPA1 and GT16a. The PCR product was sequenced and covered at least 111 bp of exon 1 and 531 bp of the promotor region. Within this sequence two different single nucleotide polymorphisms (SNP) were identified. At position –500, counting the first nucleotide preceding the published cDNA sequence [5] as –1, adenine instead of guanine was detected. Among 11 glioblastoma cell lines this polymorphism only occurred in cell line H4. This cell line, known to harbor 3 copies of chromosome 10, exhibits the polymorphism homozygous. Within 20 healthy individuals the polymorphic variant occurred once homozygously and once heterozygously, but it was not apparent in the germ line of 22 glioblastoma patients. A second polymorphism, cytosine instead of guanine at position –197, was heterozygously identified in 1 of the 20 healthy individuals, but not in the 22 analyzed glioblastoma patients or in glioma cell lines.

Sequence analysis of the *LGI1* gene has revealed a 64-bp region exhibiting characteristics of a microsatellite repeat located 0.8 kb downstream of exon 4. This region is to 84% composed of the dinucleotide TG and the largest uninterrupted repeat present in clone ICRFP700M0924Q5 consists of 13 TG repeats. PCR analysis of this repeat unveiled a heterozygosity rate of 70% in 20 healthy individuals. In the germ line of 22 glioblastoma patients we detected a heterozygosity rate of 68%. Although it is known that except T17 cells all 11 analyzed glioma-derived cell lines contain more than one copy of chromosome 10 and that the *LGI1* locus is present on every chromosome 10, all cell lines are homozygous for the analyzed microsatellite repeat. The size of the PCR product was 215 bp for clone ICRFP700M0924Q5. Mean size from healthy individuals was 209.5 bp and 210.7 bp from glioblastoma patients.

Quantification using conventional RT-PCR and measurement of band intensities

As it was evident from initial experiments that *LGI1* is expressed in 10 out of 11 cell lines, albeit mostly at very low levels, we made an attempt to gain quantitative insights into *LGI1* expression. RT-PCR analysis and subsequent densitometric quantification of LGI1 and β-actin products were used to evaluate relative expression levels. Increasing numbers of PCR cycles revealed that after 28 cycles PCR product could faintly be detected in only one cell line (Hero) as determined by gel electrophoresis. After 36 cycles there was a band seen for 6 cell lines (T17, U87-MG, T508, T1115, U373, and Hero) as shown in Fig. 5. Only after 42 cycles was there a detectable positive band for all cell lines except for H4, but with a great variation in band intensity and nonspecific co-amplification in some cell lines. Amplification of β-actin with 20 cycles revealed a homogenous positive band in all cell lines (Fig. 5). Densitometric analysis of ethidium bromide fluorescence images was used to quantify PCR products. Minimal expression was found in cell lines A172, U343, T406, and HS683, and a maximum in cell line Hero

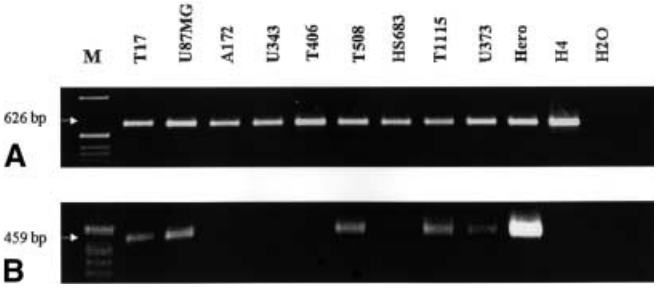

Fig. 5 PCR products of 11 glioma-derived cell lines after amplification with 20 and 36 cycles, respectively, of conventional PCR using β-actin (**A**) and LGI1 (**B**) primers [GT1s (sense) and GT2a (antisense)]. Shown are 2% agarose gels after ethidium bromide staining (*M* 1-kb DNA ladder, *H2O* negative control using water as template)

Table 4 Quantification of LGI1 mRNA expression by measurement of band intensities and after LightCycler amplification. Relative amounts of mRNA expression of all cell lines either determined by measurement of band intensity by ImageQuant software or by calculation of the corrected LGI1 concentration in relation to β-actin concentration after LightCycler amplification. Relative amount of T17 was fixed at that value and used as point of reference. Values of <0.01 after LightCycler amplification and <0.1 after measurement of band intensities were considered to be negligible, because of false-positive background measurements in the latter case. The ImageQuant value for Hero is put in parentheses as the measurement is likely to be in the saturation of the PCR, as outlined in the text

Cell line	ImageQuant LGI1/actin rel. amount	LightCycler LGI1/actin rel. amount
T17	1.0	1.0
U87-MG	0.93	0.97
A172	<0.1	<0.01
U343	<0.1	<0.01
T406	<0.1	<0.01
T508	0.99	0.26
HS683	<0.1	<0.01
T111	1.15	0.31
U373	0.26	0.06
Hero	(4.42)	588.67
H4	<0.01	<0.01

(Table 4). Cell line H4 expressed no detectable amounts of *LGI1*-mRNA. Exact quantification of relative expression levels was hampered by two intrinsic drawbacks of the method. The large differences of expression levels and the requirement for high cycle numbers in some samples may have led to an underestimation or overestimation of mRNA levels in individual cases.

Quantification using the LightCycler technology

To circumvent the drawbacks of endpoint detection by conventional PCR technology, we utilized the online detection capabilities of the LightCycler technology for more accurate quantification.

For the assessment of *LGI1* expression levels cDNA obtained from glioma-derived cell lines was amplified in the presence of specific hybridization probes utilizing the LightCycler. To normalize for sample variations *β-actin* expression was analyzed in parallel. Results were assessed by determination of the Ct, which marks the cycle count when fluorescence emission of a given sample becomes significantly different from the baseline signal, and by calculation of the resulting relative concentrations in relation to a standard dilution series. Ct for *LGI1* ranged between 25 and 45 cycles. Relative *LGI1* concentrations were normalized for β-actin signal. The resulting relative concentrations for cell line Hero was 1,000 times higher than that for the average of T17, U87-MG, U373, T508, and T1115. Cell lines A172, U343, T406, HS683, and H4 revealed even lower concentrations, almost in the range of the negative control (Table 4). Verification of amplifying

a specific product was achieved by checking the referring melting curves, showing a peak value around 67.5°C.

Retroviral gene transfer into glioma-derived cell lines

We have cloned the *LGI1* ORF into the retroviral expression vector pCFG5-IEGZ. As marker gene we chose eGFP, whose expression was coupled to the expression of LGI1 via an IRES. Coupling of marker and gene of interest allowed the fast and efficient identification and isolation of transduced cells by flow cytometry on the basis of green fluorescence. As controls, vectors carrying only the IRES-eGFP or an antisense oriented *LGI1* gene upstream of the marker gene were constructed. Gene transfer was carried out into glioblastoma cell lines T1115 and U87MG expressing low levels of endogenous *LGI1* as well as into U343 and H4 expressing barely detectable levels of *LGI1*. Gene transfer efficiencies, as judged by eGFP fluorescence, ranged between 56% and 90% for the vector harboring solely the reporter gene, and between 30% and 79% for the LGI1-IRES-eGFP vector. The vector containing the antisense-oriented *LGI1* gene was less efficient with transduction rated between 11% and 58%. We have compared growth rates of cultures after *LGI1* gene transfer to control infected cultures and could not substantiate changes in the growth rate. Cell cycle analysis by propidium iodide staining and flow cytometric analysis revealed no significant deviations in the fraction of cells undergoing S phase transition. In correspondence with these results we observed no deviations in the fraction of eGFP-expressing cells in each infected population over extended culture times. In addition, a migration assay revealed no differences between wild-type and infected cells.

Discussion

Breakpoint analysis of the t(10;19)(q24;q13) rearrangement in the human glioma cell line T98G has recently led to the isolation of a novel gene called *LGI1*, which has been located to 10q24 [5].

Analysis of mRNA expression in cell lines as well as in normal and tumor tissues revealed that *LGI1* is predominantly expressed in normal brain tissue, but is downregulated in low-grade astrocytomas and almost absent in malignant gliomas. From the localization of the *LGI1* gene and its distinctive expression in normal tissue and low- and high-grade astrocytomas, respectively, *LGI1* has been proposed to be an additional candidate TSG involved in pathogenesis of astrocytomas.

Here we have performed further characterization of the genes physical and functional properties and provide evidence that *LGI1* (1) is important in the development and maintenance of neural tissue due to its phylogenetic relationships, (2) exhibits low levels of mRNA in glioma-derived cell lines but is not a target for mutations, and (3) re-expression of the gene in vitro renders no effect.

The encoded polypeptide of the *LGI1* gene contains a hydrophobic signal peptide and a single putative transmembrane segment and is, therefore, predicted to be a membrane protein [5]. The extracellular domain is virtually exclusively composed of LRRs and cysteine-rich flanking sequences and is related to many other LRR-containing proteins [5], with the closest relationship to the neurotrophin receptors of the TRK family and proteins of the SLIT family. The intracellular domain does not show significant homologies with any other known protein domain.

A comparison of intron positions within the most closely related genes revealed a striking degree of conservation. In the majority of individual repeats accessible to analysis, the tetracosapeptide is interrupted by an intron within the highly conserved leucine at position five; 48 introns are located at this conservative position. Only within 7 repeats is the intron either absent or located at a different position. Four of these deviations are located within the last repeat of a group, which is in accordance with findings in the majority of LRR-containing proteins [3]. This high degree of structural conservation is indicative of a relationship, which has been shown previously in the analysis of small LRR proteoglycans [6].

Phylogenetic techniques are based on the quantification of sequence divergence, and distances in phylogenetic trees are related to the amount of sequence deviations [11]. Comparable strategies can be applied to predict the functions of newly identified proteins based on sequence similarities to proteins with known functions [31]. Distance matrix analysis of the LRR domains of LGI1 and members of the TRK and SLIT families uncovers a conspicuous degree of relationship. LGI1 is more closely grouped to the SLIT proteins than are members of the TRK and SLIT families. This indicates not only a high degree of sequence similarity, but, moreover, provides evidence for functional relationships.

The TRK family members are receptors for neurotrophic factors and their function is essential for development survival of neuronal cells [16]. *Drosophila slit* is a secreted protein essential for the development of central nervous system midline glia and commissural axon pathways [40]. The three identified mammalian homologues SLIT1, SLIT2 and SLIT3 are expressed in the brain, spinal chord and thyroid, respectively, and they are supposed to fulfill essential roles in development and maintenance of the nervous system [18]. The human SLIT2 protein is a functional ligand of Glypican-1, the major heparan sulfate proteoglycan of nervous tissue, and therefore is suggested to be critical for certain stages of central nervous system histogenesis [28]. The striking degree of homology between the LRR domains of LGI1, neurotrophin receptors of the TRK family and the human homologues of the *Drosophila slit* protein suggest that also LGI1 is involved in development and/or maintenance of the nervous system.

Gene transfer into glioma cell lines expressing only minute amounts of endogenous LGI1 did not influence proliferation or cell cycle distribution of transduced cells.

This indicates that this protein is not an autonomous regulator of cellular functions. The predicted structure as transmembrane protein with an extracellular domain composed almost entirely of a protein-protein interaction motif suggests that binding to some kind of ligand is essential for its biological activity. One of the most important tasks in understanding LGI1 function will be the identification of interacting partners.

LGI1 is thought to be a TSG mainly for two reasons: first, it is encoded on 10q24, a region known to frequently exhibit LOH in malignant gliomas, and it is rearranged by a translocation in cell line T98G; and second, its mRNA is rarely detectable in advanced astrocytomas.

Knowing from FISH analysis that all of our cell lines used in this study harbor at least one copy of chromosome 10, we wanted to investigate whether the 10q24, and especially the *LGI1* locus, is a target for chromosomal breakpoints or deletions. To determine the presence of the chromosomal locus of the *LGI1* gene, a locus-specific hybridization probe was used in FISH analysis. All cell lines harbored the *LGI1* locus at 10q24. Translocations of parts of chromosome 10 were detected in two of our cell lines (T406 and H4, data not shown), but *LGI1* was not involved in these derivations, suggesting that this locus might not be a frequent breakpoint. FISH analysis of the *LGI1* locus together with the *PTEN/MMAC1* locus, which is a well-characterized TSG in gliomas and is frequently deleted in high-grade astrocytomas [13, 27, 44], supports these observations.

Assuming that the genomic region is retained, it is reasonable to investigate whether the gene transcript is intact and whether the gene is expressed. We were able to amplify cDNA in ten cell lines, although, with the exception of the cell line Hero, *LGI1* seems to be expressed at very low levels. We did not find any mutation in the entire ORF in any of the ten cell lines.

Chernova et al. [5] reported that cell line A172 harbors a rearrangement affecting the *LGI1* locus. They detected no LGI1 expression in this cell line. With our methods we are not able either to prove or to exclude their interpretation of a possible inversion of the gene. However, using similar conditions in conventional RT-PCR amplification and gel electrophoresis, we were able to confirm the observation by Chernova et al. [5] and could not detect any PCR product for cell line A172 after 36 cycles (Fig. 5). However, we were able to detect a minimal amount of mRNA expression in A172 and an additional four cell lines after more than 40 PCR cycles. The minimally preserved expression suggests that at least one of the alleles has remained sufficiently intact to generate a transcript encoding the entire protein. This, in turn, might be due to the possibility that not all of the four copies of chromosome 10 are affected by a rearrangement, as has been observed by Chernova et al. [5], or there might be epigenetic mechanisms leading to a differential expression of the gene.

To achieve an estimation of the relative amount of the *LGI1* transcript, we started to measure band intensity by ImageQuant software. During the course of our experiments we noticed that accurate quantification was hampered by drawbacks of the method. Conventional endpoint analysis of DNA amplification is limited for quantification since the reaction is first exponential and finally stagnant. This precludes simultaneous analysis of samples comprising a wide range of gene expression. Therefore, high expression of *LGI1* in Hero is significantly underestimated with this technical approach. Conversely, very weak or no *LGI1* expression in certain cell lines may be overestimated.

A more accurate quantification can be achieved by online fluorescence monitoring each PCR cycle, e.g., by the recently introduced LightCycler technology [50, 51]. Amplification of *LGI1*-cDNA in the LightCycler using hybridization probes located around the start codon of the ORF resulted in different threshold cycles with a range of 20 cycles over all cell lines. We were able to reproduce these results in quintuplicate, even under varied conditions (data not shown).

Relative *LGI1* concentrations after adjustment to *β-actin* concentrations revealed extremely low copy numbers in five cell lines, which is in agreement with our findings with conventional PCR, where a product was seen only after very high cycle numbers (>40) in four cases and not detectable by that method in one case. Another five cell lines also revealed low but clearly detectable copy numbers with a mean of 0.52 (range 0.06–1.0), while one cell line, Hero, revealed a relatively high expression, which was almost three orders of magnitude higher. Particularly in the lines A172, U343, T406, HS683, and H4, where the Ct value is difficult to determine because of low copy numbers, the limits of the detection system may be reached. Analysis of melting curves confirmed the specificity of the quantified signals in all cell lines. Nevertheless, the resulting *LGI1* levels in relation to *β-actin* are almost negligible. Our findings support the observation that a diminished level of *LGI1* mRNA is a common feature in late-stage astrocytomas. However, there are large variations in the amount of mRNA expression.

Knudson [21, 22, 23] proposed a mechanism for inactivation of TSG that was popularized as “two-hit hypothesis”. *LGI1* does not seem to be a common target for the two-hit inactivation of wild-type alleles. Assuming that *LGI1* is a candidate TSG, our data supports the concept of cancer formation by reduction of TSG dosage.

However, we cannot formally rule out the possibility that mutations leading to decreased mRNA stability escaped our detection system. However, regardless of the underlying genetic and epigenetic mechanisms, this does not interfere the interpretation that *LGI1* may be a candidate TSG, because the behavior of the cell may not be influenced by the means of inactivation of a suppressor gene, but by an insufficient dosage of the wild-type protein.

The relevance of a sufficient amount of gene dosage was recently demonstrated by two reports. *PTEN/MMAC1*+/- mice developed thyroid and colon carcinomas in the presence of a remaining normal *PTEN/MMAC1* allele [7], and, the reduction of p53 levels was shown to be suffi-

cient to promote tumorigenesis in *p53*+/- mice. Fifty percent of the tumors derived from these mice were found to harbor an intact and functional *p53* allele [47]. p53 and PTEN/MMAC1 are known to be involved in glioma pathogenesis. Whether a reduced gene dosage also contributes to astrocytoma development still needs to be investigated.

With our findings that *LGI1* is present on every 10q24 in each cell line and that there is an intact transcript, if there is any measurable transcription at all, we provide evidence that *LGI1* belongs to an emerging group of genes like ZAC [2], p16 [32] or VHL [15], which are differentially inactivated.

In conclusion, we have shown that the LGI1 protein has close phylogenetic relationships to the SLIT and TRK protein family providing evidence for a function of the LGI1 protein in neural tissue. The genomic structure characterizes LGI1 as transmembrane protein. This, and the observation that overexpression of the gene in vitro does not show any effect suggest that binding of some kind of a ligand is essential for its biological activity.

The *LGI1* gene locus is present at the chromosomal level in our glioma-derived cell lines, and neither deleted nor translocated, which are events otherwise contributing to the inactivation of many TSGs. There were no mutations found in the gene transcripts, but mRNA levels were severely reduced in 10 out of 11 cell lines, suggesting that factors regulating the transcription of the gene are of pivotal importance for the inactivation of the gene during tumorigenesis.

Acknowledgements. We thank F. Zachow for careful preparation of cell lines, J. Mundt and U. Ehrenlechner for valuable assistance with the FISH analysis, and S. Faatz for critical review of the manuscript.

References

1. Altschul SF, Gish W, Miller W, Myers EW, Lipman DJ (1990) Basic local alignment search tool. J Mol Biol 215:403–410
2. Bilanges B, Varrault A, Basyuk E, Rodriguez C, Mazumdar A, Pantaloni C, Bockaert J, Theillet C, Spengler D, Journot L (1999) Loss of expression of the candidate tumor suppressor gene ZAC in breast cancer cell lines and primary tumors. Oncogene 18:3979–3988
3. Buchanan SG, Gay NJ (1996) Structural and functional diversity in the leucine-rich repeat family of proteins. Prog Biophys Mol Biol 65:1–44
4. Bunnell BA, Muul LM, Donahue RE, Blaese RM, Morgan RA (1995) High-efficiency retroviral-mediated gene transfer into human and nonhuman primate peripheral blood lymphocytes. Proc Natl Acad Sci USA 92:7739–7743
5. Chernova OB, Somerville RP, Cowell JK (1998) A novel gene, LGI1, from 10q24 is rearranged and downregulated in malignant brain tumors. Oncogene 17:2873–2881
6. Deere M, Dieguez JL, Yoon SJ, Hewett-Emmett D, De la CA, Hecht JT (1999) Genomic characterization of human DSPG3. Genome Res 9:449–456
7. Di Cristofano A, Pesce B, Cordon-Cardo C, Pandolfi PP (1998) Pten is essential for embryonic development and tumour suppression. Nat Genet 19:348–355
8. Dibb NJ, Newman AJ (1989) Evidence that introns arose at proto-splice sites. EMBO J 8:2015–2021
9. Dietmaier W, Fabry S (1994) Analysis of the introns in genes encoding small G proteins. Curr Genet 26:497–505
10. Duerr EM, Rollbrocker B, Hayashi Y, Peters N, Meyer-Puttlitz B, Louis DN, Schramm J, Wiestler OD, Parsons R, Eng C, Deimling A von (1998) PTEN mutations in gliomas and glioneuronal tumors. Oncogene 16:2259–2264
11. Felsenstein J (1996) Inferring phylogenies from protein sequences by parsimony, distance, and likelihood methods. Methods Enzymol 266:418–427
12. Feng DF, Doolittle RF (1987) Progressive sequence alignment as a prerequisite to correct phylogenetic trees. J Mol Evol 25: 351–360
13. Furnari FB, Lin H, Huang HS, Cavenee WK (1997) Growth suppression of glioma cells by PTEN requires a functional phosphatase catalytic domain. Proc Natl Acad Sci USA 94: 12479–12484
14. Herman JG (1999) Hypermethylation of tumor suppressor genes in cancer. Semin Cancer Biol 9:359–367
15. Herman JG, Latif F, Weng Y, et al (1994) Silencing of the VHL tumor-suppressor gene by DNA methylation in renal carcinoma. Proc Natl Acad Sci USA 91:9700–9704
16. Heumann R (1994) Neurotrophin signalling. Curr Opin Neurobiol 4:668–679
17. Indo Y, Mardy S, Tsuruta M, Karim MA, Matsuda I (1997) Structure and organization of the human TRKA gene encoding a high affinity receptor for nerve growth factor. Jpn J Hum Genet 42:343–351
18. Itoh A, Miyabayashi T, Ohno M, Sakano S (1998) Cloning and expressions of three mammalian homologues of Drosophila slit suggest possible roles for Slit in the formation and maintenance of the nervous system. Brain Res Mol Brain Res 62:175–186
19. Jenkins RB, Kimmel DW, Moertel CA, Schultz CG, Scheithauer BW, Kelly PJ, Dewald GW (1989) A cytogenetic study of 53 human gliomas. Cancer Genet Cytogenet 39:253–279
20. Karlbom AE, James CD, Boethius J, Cavenee WK, Collins VP, Nordenskjold M, Larsson C (1993) Loss of heterozygosity in malignant gliomas involves at least three distinct regions on chromosome 10. Hum Genet 92:169–174
21. Knudson AG Jr (1971) Mutation and cancer: statistical study of retinoblastoma. Proc Natl Acad Sci USA 68:820–823
22. Knudson AG Jr (1985) Hereditary cancer, oncogenes, and antioncogenes. Cancer Res 45:1437–1443
23. Knudson AG (1993) Antioncogenes and human cancer. Proc Natl Acad Sci USA 90:10914–10921
24. Kobe B, Deisenhofer J (1994) The leucine-rich repeat: a versatile binding motif. Trends Biochem Sci 19:415–421
25. Kreuzer KA, Lass U, Bohn A, Landt O, Schmidt CA (1999) LightCycler technology for the quantitation of bcr/abl fusion transcripts. Cancer Res 59:3171–3174
26. Leon SP, Zhu J, Black PM (1994) Genetic aberrations in human brain tumors. Neurosurgery 34:708–722
27. Li J, Yen C, Liaw D, Podsypanina K, Bose S, Wang SI, Puc J, Miliaresis C, Rodgers L, McCombie R, Bigner SH, Giovanella BC, Ittmann M, Tycko B, Hibshoosh H, Wigler MH, Parsons R (1997) PTEN, a putative protein tyrosine phosphatase gene mutated in human brain, breast, and prostate cancer. Science 275:1943–1947
28. Liang Y, Annan RS, Carr SA, Popp S, Mevissen M, Margolis RK, Margolis RU (1999) Mammalian homologues of the Drosophila slit protein are ligands of the heparan sulfate proteoglycan glypican-1 in brain. J Biol Chem 274:17885–17892
29. Lin H, Bondy ML, Langford LA, Hess KR, Delclos GL, Wu X, Chan W, Pershouse MA, Yung WK, Steck PA (1998) Allelic deletion analyses of MMAC/PTEN and DMBT1 loci in gliomas: relationship to prognostic significance. Clin Cancer Res 4:2447–2454
30. Logsdon JM Jr, Tyshenko MG, Dixon C, Jafari J, Walker VK, Palmer JD (1995) Seven newly discovered intron positions in the triose-phosphate isomerase gene: evidence for the intronslate theory. Proc Natl Acad Sci USA 92:8507–8511

31. Marcotte EM, Pellegrini M, Thompson MJ, Yeates TO, Eisenberg D (1999) A combined algorithm for genome-wide prediction of protein function. Nature 402:83–86
32. Merlo A, Herman JG, Mao L, Lee DJ, Gabrielson E, Burger PC, Baylin SB, Sidransky D (1995) 5' CpG island methylation is associated with transcriptional silencing of the tumour suppressor p16/CDKN2/MTS1 in human cancers. Nat Med 1:686–692
33. Mollenhauer J, Wiemann S, Scheurlen W, Korn B, Hayashi Y, Wilgenbus KK, Deimling A von, Poustka A (1997) DMBT1, a new member of the SRCR superfamily, on chromosome 10q25.3–26.1 is deleted in malignant brain tumours. Nat Genet 17:32–39
34. Nakamura H, Yoshida M, Tsuiki H, Ito K, Ueno M, Nakao M, Oka K, Tada M, Kochi M, Kuratsu J, Ushio Y, Saya H (1998) Identification of a human homolog of the Drosophila neuralized gene within the 10q25.1 malignant astrocytoma deletion region. Oncogene 16:1009–1019
35. Pinkel D, Straume T, Gray JW (1986) Cytogenetic analysis using quantitative, high-sensitivity, fluorescence hybridization. Proc Natl Acad Sci USA 83:2934–2938
36. Raff T, Giet M van der, Endemann D, Wiederholt T, Paul M (1997) Design and testing of beta-actin primers for RT-PCR that do not co-amplify processed pseudogenes. Biotechniques 23:456–460
37. Rasheed BK, Fuller GN, Friedman AH, Bigner DD, Bigner SH (1992) Loss of heterozygosity for 10q loci in human gliomas. Genes Chromosomes Cancer 5:75–82
38. Ririe KM, Rasmussen RP, Wittwer CT (1997) Product differentiation by analysis of DNA melting curves during the polymerase chain reaction. Anal Biochem 245:154–160
39. Robertson KD, Jones PA (2000) DNA methylation: past, present and future directions. Carcinogenesis 21:461–467
40. Rothberg JM, Jacobs JR, Goodman CS, Artavanis-Tsakonas S (1990) slit: an extracellular protein necessary for development of midline glia and commissural axon pathways contains both EGF and LRR domains. Genes Dev 4:2169–2187
41. Sano T, Lin H, Chen X, Langford LA, Koul D, Bondy ML, Hess KR, Myers JN, Hong YK, Yung WK, Steck PA (1999) Differential expression of MMAC/PTEN in glioblastoma multiforme: relationship to localization and prognosis. Cancer Res 59:1820–1824
42. Saxena A, Shriml LM, Dean M, Ali IU (1999) Comparative molecular genetic profiles of anaplastic astrocytomas/glioblastomas multiforme and their subsequent recurrences. Oncogene 18:1385–1390
43. Somerville RP, Chernova O, Liu S, Shoshan Y, Cowell JK (2000) Identification of the promoter, genomic structure, and mouse ortholog of LGI1. Mamm Genome 11:622–627
44. Steck PA, Pershouse MA, Jasser SA, Yung WK, Lin H, Ligon AH, Langford LA, Baumgard ML, Hattier T, Davis T, Frye C, Hu R, Swedlund B, Teng DH, Tavtigian SV (1997) Identification of a candidate tumour suppressor gene, MMAC1, at chromosome 10q23.3 that is mutated in multiple advanced cancers. Nat Genet 15:356–362
45. Tamura M, Gu J, Matsumoto K, Aota S, Parsons R, Yamada KM (1998) Inhibition of cell migration, spreading, and focal adhesions by tumor suppressor PTEN. Science 280:1614–1617
46. Tamura M, Gu J, Takino T, Yamada KM (1999) Tumor suppressor PTEN inhibition of cell invasion, migration, and growth: differential involvement of focal adhesion kinase and p130Cas. Cancer Res 59:442–449
47. Venkatachalam S, Shi YP, Jones SN, Vogel H, Bradley A, Pinkel D, Donehower LA (1998) Retention of wild-type p53 in tumors from p53 heterozygous mice: reduction of p53 dosage can promote cancer formation. EMBO J 17:4657–4667
48. Wechsler DS, Hawkins AL, Li X, Jabs EW, Griffin CA, Dang CV (1994) Localization of the human Mxi1 transcription factor gene (MXI1) to chromosome 10q24-q25. Genomics 21:669–672
49. Wechsler DS, Shelly CA, Petroff CA, Dang CV (1997) MXI1, a putative tumor suppressor gene, suppresses growth of human glioblastoma cells. Cancer Res 57:4905–4912
50. Wittwer CT, Herrmann MG, Moss AA, Rasmussen RP (1997) Continuous fluorescence monitoring of rapid cycle DNA amplification. Biotechniques 22:130–131, 134–138
51. Wittwer CT, Ririe KM, Andrew RV, David DA, Gundry RA, Balis UJ (1997) The LightCycler: a microvolume multisample fluorimeter with rapid temperature control. Biotechniques 22: 176–181
52. Zhou XP, Li YJ, Hoang-Xuan K, Laurent-Puig P, Mokhtari K, Longy M, Sanson M, Delattre JY, Thomas G, Hamelin R (1999) Mutational analysis of the PTEN gene in gliomas: molecular and pathological correlations. Int J Cancer 84:150–154